

Preparation, Characterization, and Performance of Tripodal Polyphosphine Rhodium Catalysts Immobilized on Silica via Hydrogen Bonding

Claudio Bianchini,^{*,†} Daryl G. Burnaby,[‡] John Evans,[‡] Piero Frediani,[§] Andrea Meli,[†] Werner Oberhauser,[†] Rinaldo Psaro,^{||} Laura Sordelli,^{||} and Francesco Vizza[†]

Contribution from the Istituto per lo Studio della Stereochimica ed Energetica dei Composti di Coordinazione (ISSECC) - CNR, Via J. Nardi 39, 50132 Firenze, Italy, Department of Chemistry, University of Southampton, Southampton, SO17 1BJ, U.K., Dipartimento di Chimica Organica, Università degli Studi di Firenze, Via G. Capponi 9, 50121 Firenze, Italy, and Centro CSSCMTBSO - CNR, Dipartimento di Chimica Inorganica, Metallorganica e Analitica, Università degli Studi di Milano, Via G. Venezian 21, 20133 Milano, Italy

Received November 12, 1998

Abstract: The heterogenization of the zwitterionic Rh(I) catalysts (sulfos)Rh(cod) (**1**) and (sulfos)Rh(CO)₂ (**2**) [sulfos = ⁻O₃S(C₆H₄)CH₂C(CH₂PPh₂)₃; cod = cycloocta-1,5-diene] is performed by controlled adsorption on partially dehydroxylated high surface area silica. The immobilization procedure is based *uniquely* on the capability of the sulfonate tail of sulfos to link the silanol groups of the support via hydrogen bonding. Experimental evidence of the ⁻SO₃⁻⋯HOSi⁻ interaction between **1** or **2** and silica has been obtained from IR, Rh K-edge EXAFS, and CP MAS ³¹P NMR studies. The grafted catalyst (sulfos)Rh(cod)/SiO₂ (**1**/SiO₂) is active for the hydrogenation of alkenes in either flow reactors (ethene, propene) or batch reactors (styrene) in hydrocarbon solvents. The hydroformylation of alkenes, here exemplified by 1-hexene, is catalyzed exclusively in solid–liquid conditions. No Rh leaching is observed in either case. In solid–gas conditions, the catalyst **1**/SiO₂ is converted by syngas to the catalytically inactive, dicarbonyl derivative (sulfos)Rh(CO)₂/SiO₂ (**2**/SiO₂). The termination metal products of the solid–gas reactions have been studied by EXAFS, while those of the batch reactions have been authenticated by NMR spectroscopy after extraction with methanol. In all of the cases investigated there was no evidence of the formation of contiguous Rh–Rh sites, indicating that the catalytic active sites are isolated Rh atoms, as in homogeneous phase. A comparison with analogous hydrogenation and hydroformylation reactions catalyzed by the soluble complex **1** in liquid–biphasic conditions shows that the immobilized catalyst is more chemoselective and more easily recyclable than the unsupported analogue.

Introduction

In a recent work, we have shown that the two mononuclear zwitterionic Rh(I) complexes (sulfos)Rh(cod) (**1**) and (sulfos)Rh(CO)₂ (**2**) [sulfos = ⁻O₃S(C₆H₄)CH₂C(CH₂PPh₂)₃; cod = cycloocta-1,5-diene] are effective catalysts for the hydrogenation of styrene to ethylbenzene and for the hydroformylation of 1-hexene to either C₇ aldehydes or C₇ alcohols in MeOH–water–hydrocarbon mixtures.¹ Complex **1** is also an efficient liquid–biphasic catalyst precursor for the hydrogenation and hydrogenolysis of benzo[*b*]thiophene to 2,3-dihydrobenzo[*b*]thiophene and 2-ethylthiophenol, respectively.² In all of these biphasic reactions,³ the rhodium complexes remain in the polar phase; the catalyst recycling and/or separation for eventual reactivation procedures, however, require a tedious and somewhat demanding manipulation under inert atmosphere. The heterogenization of **1** and **2** via tethering to stable inorganic

supports was thus seen as a viable technique to facilitate the recycling of the expensive Rh catalysts as well as to widen the range of their application to catalysis.

In this work we show that both **1** and **2** can be grafted onto a high surface area silica with an immobilization procedure based *uniquely* on the capability of the sulfonate tail of sulfos to link the silanol groups of the support via hydrogen bonding. The catalysts obtained with this technique are denoted supported hydrogen-bonded (SHB) catalysts. A similar heterogenization strategy has previously been employed for the preparation of supported transition metal oxide catalysts⁴ as well as supported aqueous phase (SAP) catalysts. These latter, however, involve the immobilization of water-soluble complexes into a thin surface water film.⁵

(3) (a) Barton, M.; Atwood, J. D. *J. Coord. Chem.* **1991**, *24*, 43. (b) Kalck, P.; Monteil, F. *Adv. Organomet. Chem.* **1992**, *34*, 219. (c) Herrmann, W. A.; Kohlpaintner, C. W. *Angew. Chem., Int. Ed. Engl.* **1993**, *32*, 1524. (d) Horváth, I. T., Joó F., Eds. *Aqueous Organometallic Chemistry and Catalysis*; Kluwer: Dordrecht, The Netherlands, 1995. (e) Papadogianakis, G.; Sheldon, R. A. *New J. Chem.* **1996**, *20*, 175. (f) Joó, F.; Kathó, A. *J. Mol. Catal.* **1997**, *116*, 3. (g) *Aqueous-Phase Organometallic Catalysis – Concepts and Applications*; Cornils, B., Herrmann, W. A., Eds.; VCH: Weinheim, Germany, 1998.

(4) Van der Voort, P.; Possemiers, K.; Vansant, E. F. *J. Chem. Soc., Faraday Trans.* **1996**, *92*, 843, and references therein.

[†] ISSECC-CNR.

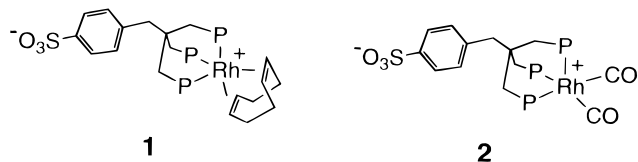
[‡] University of Southampton.

[§] Università di Firenze.

^{||} Centro CNR CSSCMTBSO.

(1) Bianchini, C.; Frediani, P.; Sernau, V. *Organometallics* **1995**, *14*, 5458.

(2) Bianchini, C.; Meli, A.; Patinec, V.; Sernau, V.; Vizza, F. *J. Am. Chem. Soc.* **1997**, *119*, 4945.



Experimental evidence of the $-\text{SO}_3\cdots\text{HOSi}-$ interaction between **1** or **2** and silica has been obtained from IR, Rh K-edge EXAFS, and CP MAS ^{31}P NMR studies.

In an attempt to provide information on the reactivity of isolated Rh(I) surface sites in catalytic conditions,⁶ the potential of the supported complexes **1**/ SiO_2 and **2**/ SiO_2 has been scrutinized for the solid–gas hydrogenation and hydroformylation of ethene and propene as well as the batch hydroformylation of 1-hexene and the hydrogenation of styrene in hydrocarbon solvents. All of the reactions attempted were successfully accomplished with the exception of the solid–gas hydroformylation of the alkenes.

Experimental Section

General Information. All reactions and manipulations were routinely performed under a nitrogen or argon atmosphere by using standard Schlenk techniques. CH_2Cl_2 was distilled from CaH_2 . All of the other reagents and chemicals were reagent grade and were used as received by commercial suppliers. The rhodium complexes **1** and **2** were prepared as previously described.¹ Deuterated solvents for NMR measurements (Merck or Cortec) were dried over molecular sieves. Batch reactions under a controlled pressure of gas were performed with a stainless steel Parr 4565 reactor (100 mL) equipped with a Parr 4842 temperature and pressure controller. GC analyses of the solutions were performed on a Shimadzu GC-14 A gas chromatograph equipped with a flame ionization detector and a 30 m (0.25 mm id, 0.25 μm film thickness) SPB-1 Supelco fused silica capillary column. A UCON-oil LB 550-X packed column (PPG, 2 m, $1/8$ in. id) was employed for the determination of hydrocarbons, 2-ethylpentanal, 2-methylhexanal, and heptanal. An Al_2O_3 –PLOT capillary column (50 m, 0.32 mm id) was employed for the determination of hexane, 1-hexene, cis- and trans-2-hexene, and cis- and trans-3-hexene. GC/MS analyses were performed on a Shimadzu QP 5000 apparatus equipped with a SPB-1 Supelco fused silica capillary column. Atomic absorption analyses were carried out with a Perkin-Elmer 400 instrument at a sensitivity level of 1 ppm. The Davison 62 silica employed in this work is a high surface area ($S_{\text{BET}} = 357 \text{ m}^2/\text{g}$), hydrophilic mesoporous material, with a narrow pore size distribution ($\bar{\phi} = 13.8 \text{ nm}$). The pore volume is $1.23 \text{ cm}^3/\text{g}$ as determined by adsorption of nitrogen at 77 K. The support was ground, washed with 1 M HNO_3 and then with distilled water to neutrality, and dried overnight in an oven at 100°C . Solid–gas reactions at atmospheric pressure were performed in a fixed-bed, continuous flow glass microreactor interfaced to a HP5890A GC (FID detector). Product analyses were performed with a Porapack Q25 column (25 m, 0.53 mm id).

Impregnation Methodology. Samples of (sulfos)Rh(cod)/ SiO_2 (**1**/ SiO_2) and (sulfos)Rh(CO)₂/ SiO_2 (**2**/ SiO_2) were prepared by the solvent impregnation method.⁷ The silica was pretreated in air at 300°C for 3 h and then left under vacuum (10^{-5} Torr) for a further 16 h at 300°C . By this procedure, the adsorbed water was removed from the silica surface with a weight loss of 12% as determined by TGA. In a typical experiment, the rhodium precursor was stirred in anhydrous CH_2Cl_2 at room temperature under Ar until a clear, yellow solution was obtained.

(5) (a) Arhancet, J. P.; Davis, M. E.; Merola, J. S.; Hanson, B. E. *Nature* **1989**, 339, 454. (b) Arhancet, J. P.; Davis, M. E.; Merola, J. S.; Hanson, B. E. *J. Catal.* **1990**, 121, 327. (c) Arhancet, J. P.; Davis, M. E.; Hanson, B. E. *J. Catal.* **1991**, 129, 94. (d) Davis, M. E. *CHEMTECH* **1992**, August, 498.

(6) (a) van't Bilk, H. F.; van Zon, A. D.; Huizinga, T.; Vis, J. C.; Koningsberger, D. C.; Prins, R. *J. Am. Chem. Soc.* **1985**, 107, 3139. (b) Iwasawa, Y. in *Dynamic Processes on Solid Surfaces*; Tamaru, K., Ed.; Plenum Press: New York, 1993; p 91.

(7) Komiyama, M. *Catal. Rev.* **1985**, 27, 341.

To this solution was added the silica with stirring. Stirring was maintained for 6 h at room temperature. After this time, the silica assumed a yellow color while the solution became colorless.

The separation of the grafted material was performed with a Pyrex büchner filtering funnel under Ar. Once separated as yellow powders, the solid products were maintained under vacuum (10^{-3} Torr) overnight at room temperature and, afterward, stored under Ar prior to use. With this procedure, catalysts with metal loadings up to 2 wt % were obtained in a reproducible way. The Rh contents were determined by atomic absorption spectroscopy. Each sample (70 mg) was treated in a microwave heated digestion bomb (Milestone, MLS-200) with concentrated HNO_3 (3 mL), 98% H_2SO_4 (3 mL), and a pellet (1 g) of a digestion aid reagent (0.1% Se in K_2SO_4). After the silica particles were filtered off, the solutions were analyzed. The addition of selenium was necessary to get an effective digestion of the phosphine ligand, which was hardly achievable by usual acid dissolution procedures. Moreover, the high potassium concentration from the pellet, acting as an ionization suppressor toward rhodium, contributed to an enhancement of the signal in the atomic absorption measurements.

IR Spectroscopy. Spectra were recorded on a Digilab FTS-40 instrument equipped with a KBr beam splitter and a DTGS detector operating between 400 and 4000 cm^{-1} . The spectra were recorded in transmission on wafers obtained by pressing in air the silica powder at 5 ton cm^{-2} (18 mm in diameter, 50 mg). The wafers were placed in an especially designed T-shaped Pyrex cell equipped with CaF_2 windows. This cell allows one to carry out thermal treatments as well as to operate in a vacuum or under a controlled atmosphere.⁸ The silica wafers were pretreated according to the procedure reported in the impregnation method and then impregnated in situ with a CH_2Cl_2 solution of **2** under Ar to give about a 1% Rh concentration by weight. The spectra were recorded with a resolution of 4 cm^{-1} and the coaddition of 128 scans; the spectrum of the support just before the impregnation was adopted as background.

Temperature-Programmed Decomposition Studies. The thermal decomposition of **1**/ SiO_2 was studied by temperature-programmed reductive decomposition (TPRD). The catalyst (100 mg) was placed in a Pyrex fixed-bed flow reactor on a glass frit and heated in a flowing gas mixture of H_2 (5%)–He from 20 to 300°C at a heating rate of $3^\circ\text{C}/\text{min}$. The volatile decomposition products were detected downstream in the carrier gas with the temperature by an on-line quadrupole mass spectrometer. The apparatus is described elsewhere.⁹ The choice of the mass channels to be monitored was made on the basis of the standard mass spectra, available in the literature.

EXAFS Experiments. X-ray absorption spectra were collected either at Station 9.2 at the CLRC Daresbury Laboratory Source Synchrotron Radiation operating at 2 GeV electron energy and at a storage ring current of 200 mA, with a Si(220) double crystal monochromator, or at the GILDA station at the ESRF (Grenoble) with a Si(311) double crystal monochromator. Harmonic rejection was achieved in both cases by a 50% detuning of the two Si crystals. Rh metal foil has been used for the angle/energy calibration. Spectra were recorded at 300 K in fluorescence mode at the 9.2 station and in the transmission mode at GILDA, at the Rh K-edge over the range 23–24.2 keV, with an energy sampling step of 1–2 eV and an increasing integration time from 2 to 16 s per point. Incident and transmitted photon fluxes have been detected with a ionization chamber filled with 0.1 bar of Kr, and fluorescence photons were analyzed with a 13-element Germanium Canberra detector. Each spectrum has been acquired three times. The pure samples were ground up with boron nitride prior to recording the spectra, to give a metal content in them of approximately 10%. The powder supported samples were loaded under inert atmosphere, reacted in situ in a catalysis EXAFS cell (Lytle type for transmission and for fluorescence a new cell has been developed^{10a}), and cooled to room

(8) Psaro, R.; Ugo, R.; Zanderighi, G. M.; Besson, B.; Smith, A. K.; Basset, J. M. *J. Organomet. Chem.* **1981**, 213, 215.

(9) Dossi, C.; Psaro, R.; Bartsch, A.; Brivio, E.; Galasco, A.; Losi, P. *Catal. Today* **1993**, 17, 527.

(10) (a) Rudkin, C. J., Ph.D. Thesis, University of Southampton, 1997. (b) Binsted, N. *PAXAS Programme for the Analysis of X-ray Absorption Spectra*; University of Southampton: Southampton, U.K., 1988. (c) Lengeler, B.; Eisenberger, E. P. *Phys. Rev. B* **1980**, 21, 4507.

temperature before spectra acquisition. Extracted $\chi(k)$ data have been averaged before the EXAFS data analysis. Experimental $\chi(k)$ data were extracted from absorption data with the PAXAS program,^{10b} whose procedure is outlined as follows: a polynomial background was fitted in the pre-edge region, extrapolated to higher energies, and then subtracted from absorption data. The atomic-like contribution was estimated by a polynomial fit and then subtracted from experimental data following the procedure proposed by Lengeler and Eisenberger.^{10c} The result was normalized to edge height to obtain experimental $\chi(k)$ values. The spherical wave curve-fitting analysis was performed by least-squares refinement of non Fourier-filtered $\chi(k)$, using the EX-CURVE program (developed by Gurman and Binsted),¹¹ using Van-Barth ground-state potentials and Hedin-Lundquist exchange potentials. The k^3 -weighted $\chi(k)$ data, Fourier transformed over a Kaiser window in a typical k range of 3–14 Å⁻¹, are reported in all plots together with the phaseshift-corrected theoretical best fits.

NMR Spectroscopy. Liquid-phase ¹H (200.13 MHz), ¹³C{¹H} (50.32 MHz), and ³¹P{¹H} (81.01 MHz) NMR spectra were obtained on a Bruker ACP 200 spectrometer. All chemical shifts are reported in parts per million (δ) relative to tetramethylsilane, referenced to the chemical shifts of residual solvent resonances (¹H, ¹³C) or 85% H₃PO₄ (³¹P). Solid-state ³¹P NMR spectra were recorded at room temperature on a Bruker AMX 300 WB spectrometer equipped with a 4 mm BB-CP MAS probe at a working frequency of 121.50 MHz. The spectra were recorded using the cross polarization pulse sequence¹² under magic angle spinning at a spinning rate of 10 kHz at room temperature. The 90° pulse was 3.9 μ s, and the contact pulse was 1 ms. In the case of **1**, the spectra were collected after 80 scans using a recycle time of 10 s, while the spectrum of the supported complex **1**/SiO₂ was acquired with 8000 scans and a relaxation delay of 1 s. The line broadening was set to be 10 Hz for **1** and 100 Hz for **1**/SiO₂. H₃PO₄ (85%) was used as the external standard. The samples were transferred in the rotor in a dry glovebox under N₂.

Solid-Gas Reactions: Hydrogenation and Hydroformylation of Ethene, Propene. A fixed-bed glass microreactor was charged with **1**/SiO₂ (300 mg) and then heated for 1 h to 120 °C in a flow of Ar. Following this activation procedure, the hydroformylation and hydrogenation reactions were carried out at 120 °C and atmospheric pressure (CO–H₂–alkene = 1:1:1; H₂–alkene = 1:1). No catalytic activity was observed even after 20 h on stream. A fresh catalyst was then heated in situ for 1 h at 150 °C in a flow of H₂. After the temperature was decreased to 120 °C in either H₂ or Ar flow, the catalysts were highly active for the hydrogenation of alkenes, while they were totally inactive in the presence of syngas.

Batch Reactions: Hydrogenation of Styrene. A 100 mL Parr autoclave was charged with **1**/SiO₂ (113.2 mg, 0.022 mmol Rh), styrene (0.25 mL, 2.20 mmol), *n*-octane (30 mL), and H₂ (30 bar). The ensemble was heated to 120 °C and then stirred (1500 rpm) for 3 h, after which the vessel was cooled to ambient temperature and the liquid contents analyzed by GC to reveal 100% conversion to ethylbenzene. The stability of the immobilized catalyst against leaching from the support was tested as follows. (i) The grafted Rh product was separated by filtration from the liquid phase under nitrogen, washed with *n*-octane and CH₂Cl₂, and then reused for a second, identical run which gave total conversion of styrene to ethylbenzene. Most of the *n*-octane solvent was removed from the liquid phase under vacuum, and the residue was analyzed by both ³¹P{¹H} NMR spectroscopy and atomic absorption spectrophotometry. In no case was an appreciable trace of phosphorus or rhodium detected (at a sensitivity level of 1 ppm). Atomic absorption analyses showed that the Rh contents in the tethered termination products were always substantially similar to those in the unreacted precursors. (ii) After a catalytic run, the contents of the reactor were filtered at 120 °C through a sintered glass frit (0.7- μ m pores) and the filtrate (ca 20 mL) was transferred into a Parr reactor containing 0.2 mL of styrene immersed into an ice–water bath. After being pressurized with H₂ to 30 bar, the solution was heated to 120 °C for 3

h. The conversion of styrene into ethylbenzene was comparable to those obtained in blank tests (<1%).

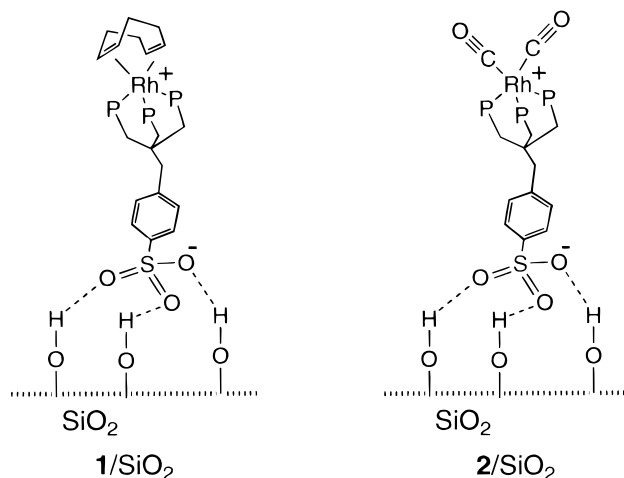
In a separate experiment, finely crushed **1** was used also as catalyst precursor in the place of the supported species **1**/SiO₂. No hydrogenation of styrene was observed under comparable reaction conditions.

Hydroformylation of 1-Hexene. A 100 mL Parr autoclave was charged with **1**/SiO₂ (113.2 mg, 0.022 mmol Rh) and 1-hexene (0.25 mL, 2.20 mmol) in *i*-octane (30 mL). The autoclave was pressurized to 30 bar with a 1:1 syngas mixture and then heated to 120 °C with stirring (300 rpm). After 3 h, the vessel was cooled to ambient temperature and the liquid contents were analyzed by GC to reveal that all of the substrate had disappeared. The following product composition was determined at 100% conversion: heptanal (32.0%), 2-methylhexanal (41.0%), 2-ethylpentanal (15.5%), *cis*-2-hexene (1.5%), *trans*-2-hexene (4.5%), *cis*-3-hexene (0.5%), *trans*-3-hexene (1.5%), and hexane (3.5%). The stability of the hydroformylation catalyst against leaching was tested as described above for the hydrogenation of styrene. No appreciable rhodium leaching was found.

Results and Discussion

Synthesis of the Grafted Complexes. The impregnation solvent of choice was anhydrous dichloromethane for its aprotic nature and its capability to dissolve appreciable amounts of (sulfos)Rh(cod) (**1**) and (sulfos)Rh(CO)₂ (**2**). Alcohols cannot be used as they compete with the Rh complexes for interaction with the silica surface.¹³

The first indication that the formation of the supported species **1**/SiO₂ and **2**/SiO₂ (see sketches below) was dependent on the



hydroxyl coverage of silica was provided by the fact that the chemisorption process was limited to 65% when a rehydrated silica surface was used. For a thermal pretreatment at 300 °C,¹⁴ needed to remove the physisorbed water from the support, the grafting procedure was complete and reproducible up to 2 wt % Rh loading.

Effective OH consumption during the chemisorption process was indeed evident from the IR studies carried out on wafers. In Figure 1 are reported the IR spectra in the ν (OH) region. After the thermal pretreatment of the silica surface, the hydroxyl groups characterized by the band at 3747 cm⁻¹ (Figure 1b) were isolated silanols.¹⁵ Adsorption of **2** (Figure 1a) significantly reduced the intensity of this IR band, as is evident from the

(13) Borrello, E.; Zecchina, A.; Morterra, A. *J. Phys. Chem.* **1967**, *71*, 2938.

(14) The Davison silica surface was treated at 300 °C to control the concentration of the surface isolated OH groups at ca. 1.8 OH/nm². See the following: (a) Zhuravlev, L. T. *Colloids Surf.* **1993**, *74*, 71. (b) Basu, P.; Panayotov, D.; Yates, J. T. Jr. *J. Am. Chem. Soc.* **1988**, *110*, 2074.

(15) Hair, M. L. *Infrared Spectroscopy in Surface Chemistry*, Marcel Dekker: New York, 1967; p 79.

(11) (a) Gurman, S. J.; Binsted, N.; Ross, J. J. *J. Phys. Chem.* **1984**, *88*, 143. (b) Gurman, S. J.; Binsted, N.; Ross, J. J. *J. Phys. Chem.* **1986**, *90*, 1845.

(12) Pines, A.; Gibby, M. G.; Waugh, J. S. *J. Chem. Phys.* **1972**, *56*, 776.

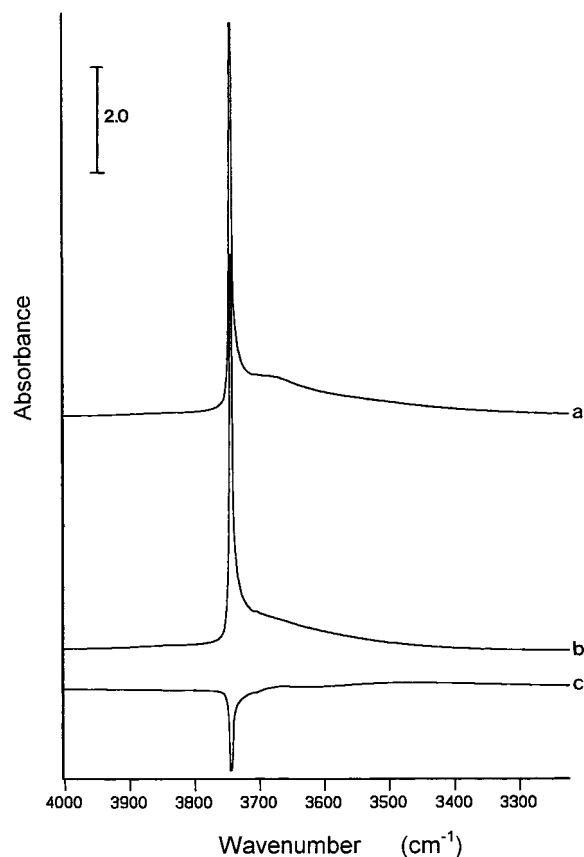


Figure 1. IR spectra in the $\nu(\text{OH})$ region of (a) $2/\text{SiO}_2$ just impregnated; (b) activated silica just before complex impregnation; and (c) difference spectrum $a - b$.

Table 1. Infrared Stretching Frequencies in the Carbonyl Region for **2**

	$\nu(\text{CO}), \text{cm}^{-1}$	
CH_2Cl_2	2060	1993
EtOH	2058	1991
KBr ^a	2049	1979
SiO_2^b	2058	1991

^a Solid state as a KBr pellet. ^b Grafted on SiO_2 wafer.

difference spectrum reported in Figure 1c. A broad band centered at 3675 cm^{-1} in the spectrum of the anchored complex (Figure 1a) can be assigned to the silanols in hydrogen interaction with the sulfonate group.^{4,5,15}

Once grafted to silica, the Rh complexes were not extracted back into CH_2Cl_2 solutions even after repeated washings with this solvent. In contrast, stirring $1/\text{SiO}_2$ and $2/\text{SiO}_2$ in MeOH or EtOH for 3 h at room temperature resulted in the complete delivery of the complexes into solution (^{31}P NMR experiments in MeOH- d_4 , vide infra).

Following an identical impregnation procedure, the heterogenization of $[(\text{triphos})\text{Rh}(\text{cod})]\text{PF}_6$ did not occur.

Characterization of the Grafted Complexes: Infrared Spectra. A detailed IR study was carried out for both **2** and the corresponding silica-grafted species $2/\text{SiO}_2$ just to use the stretching modes of the geminal carbonyl groups as an internal probe of the interaction with the support.

The stretching frequencies of the carbonyl ligands in **2**,¹ dissolved in different solvents or in the solid state in different media, are reported in Table 1.

In solution, the $\nu(\text{CO})$ bands for the two coordinatively inequivalent *cis*-disposed CO ligands are shifted to higher energy

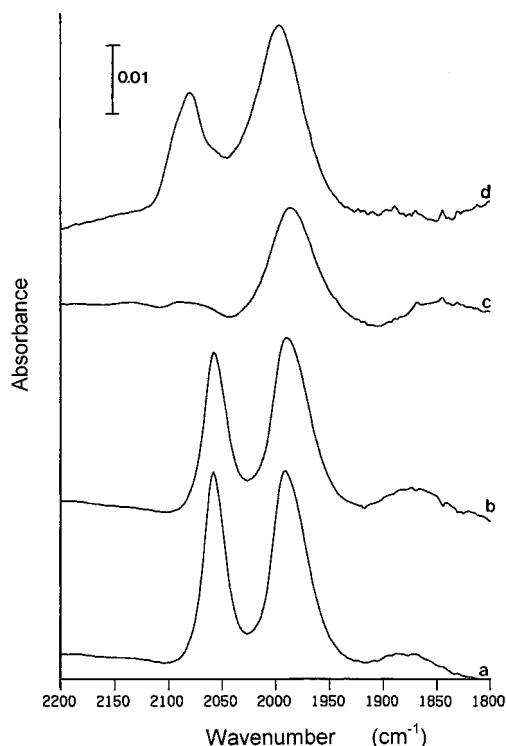


Figure 2. IR spectra in the $\nu(\text{OH})$ region of $2/\text{SiO}_2$ (a) after 10 min of outgassing after impregnation at 25°C ; (b) after 2 h under vacuum at 25°C ; (c) after 16 h under vacuum at 120°C ; and (d) after 1 h under CO atmosphere at 25°C .

by $\sim 10\text{--}13 \text{ cm}^{-1}$ as compared to solid state. This finding is quite interesting as the analogous bands for $2/\text{SiO}_2$ (Figure 2a) are just coincident with those of the solution spectra of **2**, which not only shows that after impregnation no relevant perturbation of the Rh coordination sphere occurs but also suggests that the grafted complex is well separated from other complex molecules as occurs in solution. A similar molecularly dispersed state has previously been observed for $\text{Os}_3(\text{CO})_{12}$ and $\text{Ir}_4(\text{CO})_{12}$ physisorbed on SiO_2 .¹⁶

After 2 h under high vacuum to remove eventual residual solvent, the IR spectrum of $2/\text{SiO}_2$ in the $\nu(\text{CO})$ region was unchanged with bands at 2058 and 1991 cm^{-1} (Figure 2b). A subsequent treatment of the grafted dicarbonyl complex under vacuum at 120°C overnight caused the disappearance of the high-frequency band and also shifted the lower-frequency band to 1987 cm^{-1} (Figure 2c). A re-exposure of the sample to a CO atmosphere regenerated the two bands, both at slightly higher frequency (2079 and 1996 cm^{-1}), however (Figure 2d). This behavior is apparently suggestive of the existence of an equilibrium between mono- and dicarbonyl-grafted species, depending on the CO pressure and temperature. The true nature of eventual carbonyl-deficient species is difficult to determine. Moreover, the broad appearance of the CO stretching absorptions during the decarbonylation/carbonylation experiment suggests that structurally different species may also be present. No loss of CO was detected under high vacuum at room temperature, while the spectrum did not change by heating the sample at 120°C under a dinitrogen or argon atmosphere.

Interestingly, no significant variation in the $\nu(\text{CO})$ region of the IR spectrum was observed when the sample was heated under an O_2 atmosphere even for 2.5 h at 120°C (Figure 3b).

(16) (a) Dossi, C.; Psaro, R.; Roberto, D.; Ugo, R.; Zanderighi, G. M. *Inorg. Chem.* **1990**, *29*, 4368. (b) Psaro, R.; Dossi, C.; Fusi, A.; Della Pergola, R.; Garlaschelli, L.; Roberto, D.; Sordelli, L.; Ugo, R.; Zani, R. *J. Chem. Soc., Faraday Trans.* **1992**, *88*, 369.

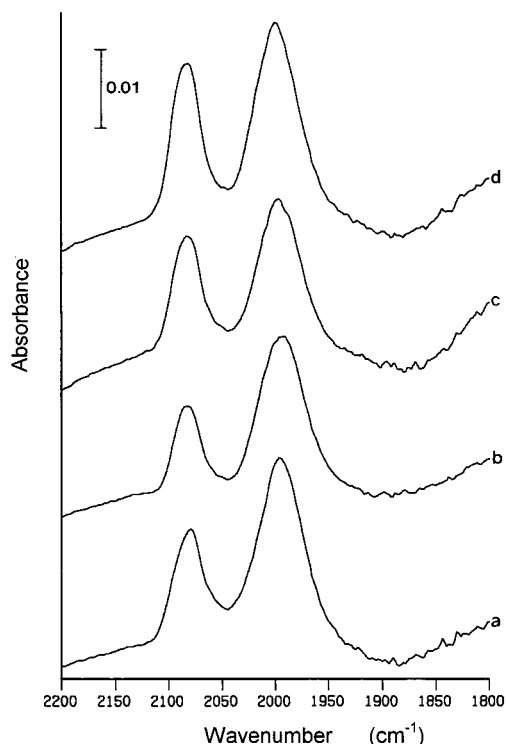


Figure 3. IR spectra in the $\nu(\text{CO})$ region of $2/\text{SiO}_2$ (a) after 1 h under O_2 at 50 °C; (b) after 2.5 h under O_2 at 120 °C; (c) after 16 h under CO at 25 °C; and (d) after 2.5 h under CO at 120 °C.

The remarkable stability toward O_2 exhibited by $2/\text{SiO}_2$ contrasts with the facile decomposition of the cod derivative $1/\text{SiO}_2$ in comparable conditions. Indeed, the formation of phosphine oxide species (detected by ^{31}P NMR spectroscopy in either the solid state or the solution after extraction with MeOH-d_4) occurs, although slowly, upon exposure of $1/\text{SiO}_2$ to air even at room temperature. This different reactivity of $1/\text{SiO}_2$ and $2/\text{SiO}_2$ may reasonably be interpreted in terms of a stronger coordination of the CO ligands to Rh as compared to cod; it also suggests that the oxidation of the phosphorus donors to phosphine oxide implies a vacant site at rhodium for the activation of O_2 .¹⁷ In the solid state, the creation of a free coordination site is evidently easier for the cod ligand that may unfasten an olefinic end¹⁸ than for the dicarbonyl complex which liberates a CO molecule only if subjected to high vacuum at high temperature (≥ 120 °C).

A re-exposure of $2/\text{SiO}_2$ to CO at room temperature after the treatment with oxygen resulted in a modest increase in the intensity of the higher-frequency carbonyl band (Figure 3c). The same effect was also noticed when the sample was heated to 120 °C for 2.5 h under CO (Figure 3d).

NMR Spectra. In CD_2Cl_2 solution, the $^{31}\text{P}\{^1\text{H}\}$ NMR spectrum of **2** consists of a doublet at δ 6.6 ($J(\text{PRh}) = 98.0$ Hz) invariant with the temperature down to -100 °C.¹ A doublet resonance features also the $^{31}\text{P}\{^1\text{H}\}$ NMR spectrum of **1** (δ 5.8, $J(\text{PRh}) = 104.5$ Hz) in the temperature range from 30 to -60 °C.¹ We have now found that, below -60 °C, the doublet resonance due to **1** broadens and then coalesces at -70 °C. For a further decrease of the temperature down to -100 °C, two broad signals with no discernible P–P or P–Rh couplings emerge from the baseline with chemical shifts of $\delta \sim 9$ and -1.0

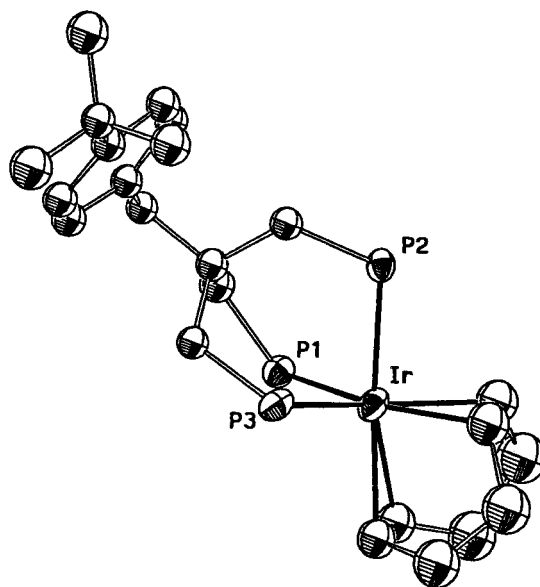


Figure 4. ORTEP drawing of (sulfos)Ir(cod). All of the hydrogen atoms and phenyl substituents at the phosphorus atoms of triphos are omitted for clarity. Selected bond lengths (Å) are the following: Ir–P1, 2.367(3); Ir–P2, 2.324(3); Ir–P3, 2.374(3); Ir–C, 2.172(14), 2.170(15), 2.236(13); 2.253(13).

in an $\sim 2:1$ ratio. The overall appearance of this sequence of variable-temperature spectra is typical of five-coordinate metal complexes with the ligand triphos.¹⁹ In particular, the magnetic equivalence of the three phosphorus atoms in the fast-exchange regime (A_3 pattern) has been related to a fast rearrangement between square-pyramidal (SQ) and trigonal-bipyramidal (TBP) structures.^{19,20b} In the slow motion regime, either of these limiting structures would give rise to an AM_2 pattern which can only be envisaged in the ^{31}P spectrum of **1** at -100 °C. Due to the geometrical constraints of the tripodal ligand, no five-coordinate metal complex with triphos can assume a perfect SQ or TBP conformation in the solid state; the complexes invariably adopt more or less distorted geometries depending on the coligands.^{19,20} Unfortunately, we were unable to grow crystals of either **1** or **2** suited for an X-ray analysis and thus we cannot assign a preferential coordination geometry to either complex in the solid state. A distorted TBP structure has been determined, however, for the iridium derivative (sulfos)Ir(cod), which has been characterized by X-ray methods (Figure 4).²¹

On the basis of the CP MAS ^{31}P NMR spectrum shown in Figure 5, the Rh congener **1** may tentatively be assigned a structure closer to a square-pyramid than to a trigonal-bipyramid. The ^{31}P NMR spectrum contains three phosphorus resonances at δ 23.8, 0.5, and -3.5 for an δ_{av} of ~ 6.9 not too far from the

(19) (a) Ott, J.; Venanzi, L. M.; Ghilardi, C. A.; Midollini, S.; Orlandini, A. *J. Organomet. Chem.* **1985**, *291*, 89. (b) Dahlenburg, L.; Mirzaei, F. *Inorg. Chim. Acta* **1985**, *97*, L1. (c) Johnson, G. G.; Baird, M. C. *Organometallics* **1989**, *8*, 1894. (d) Bianchini, C.; Meli, A.; Peruzzini, M.; Vizza, F.; Frediani, P.; Ramirez, J. A. *Organometallics* **1990**, *9*, 226. (e) Bianchini, C.; Meli, A.; Peruzzini, M.; Vacca, A.; Vizza, F. *Organometallics* **1991**, *10*, 645.

(20) (a) Bachechi, F.; Ott, J.; Venanzi, L. M. *Acta Crystallogr., Sect. C* **1989**, *45*, 724. (b) Thaler, E. G.; Foltling, K.; Caulton, K. G. *J. Am. Chem. Soc.* **1990**, *112*, 2664. (c) Bianchini, C.; Frediani, P.; Herrera, V.; Jiménez, M. V.; Meli, A.; Rincón, L.; Sánchez-Delgado, R.; Vizza, F. *J. Am. Chem. Soc.* **1995**, *117*, 4333. (d) Scherer, J.; Huttner, G.; Walter, O.; Janssen, B. C.; Zsolnai, L. *Chem. Ber.* **1996**, *129*, 1603.

(21) Bianchini, C. et al., X-ray crystal structure of (sulphos)Ir(cod), manuscript in preparation. Crystal data: space group $P2_1/c$, monoclinic; $a = 17.892(5)$, $b = 11.025(5)$, $c = 24.885(5)$ Å; $\alpha = 90.005(5)$, $\beta = 93.440(5)$, $\gamma = 90.000(5)^\circ$; $V = 4900(3)$ Å³; $d_{\text{calcd}} = 1.464$ g cm⁻³; $Z = 4$; $R[I > 2\sigma(I)] = 0.060$, $R(\text{all data}) = 0.1051$.

(17) Bianchini, C.; Mealli, C.; Meli, A.; Proserpio, D. M.; Peruzzini, M.; Vizza, F. *J. Organomet. Chem.* **1989**, *369*, C6.

(18) Bianchini, C.; Farnetti, E.; Graziani, M.; Nardin, G.; Vacca, A.; Zanobini, F. *J. Am. Chem. Soc.* **1990**, *112*, 9190.

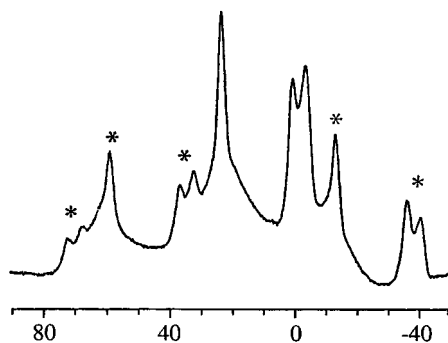


Figure 5. CP MAS ^{31}P NMR spectrum of **1**. Spinning sidebands are denoted by asterisks.

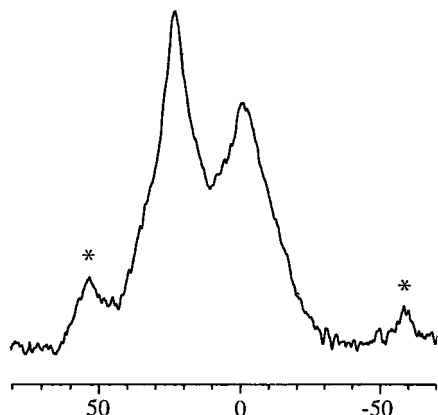


Figure 6. CP MAS ^{31}P NMR spectrum of **1/SiO₂**. Spinning sidebands are denoted by asterisks.

solution shift (δ 5.8) given the sensitivity of the ^{31}P shifts to solvent and temperature. In SQ geometry, the peak at lowest field (δ 23.8) can be assigned to the axial P atom which has no trans olefinic ligands.

The CP MAS ^{31}P NMR spectrum of the grafted complex **1/SiO₂** is shown in Figure 6 and consists of two signals centered at δ 23.7 and -2.1 . The asymmetric profile of the latter peak indicates that different types of phosphorus may be present. Despite the expected shift dispersion and line broadening as compared to the unsupported sample,²² the solid-state NMR spectra of **1/SiO₂** and **1** are substantially similar and thus consistent with the immobilization of the cod complex on the silica through a functional group away from the metal coordination sphere.

EXAFS Studies. EXAFS studies have been carried out for the cod complex as either pure compound (**1**) or silica-supported species (**1/SiO₂**). To better resolve the structure of the complex EXAFS signal, to which multiple shell and scattering contribute, we have analyzed various reference Rh compounds of known crystallographic structure containing either triphenylphosphine and/or cod ligands. In the figures, solid lines represent experimental data, while the dashed lines show the phaseshift-corrected theoretical model.

Table 2 reports the best-fit parameter values obtained from the EXAFS spectra for Rh foil, $\text{RhCl}(\text{PPh}_3)_3$, and $[\text{Rh}(\text{cod})\text{Cl}]_2$ as well as selected crystal structure data. The Rh–P and Rh–Cl bond lengths for the Wilkinson's catalyst are in close agreement with the crystal structure.²³ A good fit between

(22) Beml, L.; Clark, H. C.; Davies, J. A.; Fyfe, C. A.; Wasylishen, R. E. *J. Am. Chem. Soc.* **1982**, *104*, 438.

(23) (a) Hitchcock, P. B.; McPartlin, M.; Mason, R. *J. Chem. Soc., Dalton Trans.* **1969**, 1367. (b) Albano, V. G.; Bellon, P.; Sansoni, M. *J. Chem. Soc. A* **1971**, 2429. (c) Bennett, M. J.; Donaldson, P. B. *Inorg. Chem.* **1977**, *16*, 655.

Table 2. Crystallographic Parameters of Reference Compounds Used for Experimental Phase and Amplitude Extraction

sample	atom	CN ^a	r (Å) ^b	X-ray bond length (Å)	2σ ² (Å ²) ^c
Rh foil	Rh	12	2.676(1)	2.69	0.007(1)
	Rh	6	3.784(4)	3.80	0.011(1)
	Rh	24	4.652(3)	4.66	0.012(1)
	Rh	12	5.262(3)	5.38	0.004(1)
$\text{RhCl}(\text{PPh}_3)_3$	P	3	2.262(2)	2.310	0.007(4)
	Cl	1	2.366(2)	2.377	0.001(4)
	C	4	3.32(1)	3.300	0.01(3)
	C	5	3.65(2)	3.650	0.02(5)
$[\text{Rh}(\text{cod})\text{Cl}]_2$	C	4	2.105(1)	2.106	0.006(2)
	Cl	2	2.403(1)	2.399	0.008(2)
	C	4	3.049(1)	3.051	0.010(9)
	Rh	1	3.516	3.509	0.014(9)

^a Coordination number. ^b Interatomic distance. ^c Debye-Waller factor, σ = root-mean-square internuclear separation.

Table 3. Curve-Fitting Results of the Rh K-Edge EXAFS Data

sample	atom	CN ^a	r (Å) ^b	2σ ² (Å ²) ^c	R (%) ^d	E _f (eV)
a 1	C	4	2.135(3)	0.011(5)	18.27	-1.17
	P	3	2.363(2)	0.010(2)		
	C	4	3.141(9)	0.02(2)		
	C	5	3.56(1)	0.018(4)		
b 1/SiO₂	C	4	2.05(1)	0.017(3)	31.26	7.23
	P	3	2.265(6)	0.014(1)		
c 1/SiO₂ (H ₂ 150 °C)	P	3	2.343(5)	0.021(1)	47.15	-5.21
	C	4	2.907(5)	0.007(1)		
d 1/SiO₂ (H ₂ -C ₂ H ₄ 120 °C)	C	1	2.111(7)	0.001(1)	53.12	-1.33
	P	3	2.33(1)	0.026(2)		
	C	1	2.585(9)	0.002(1)		
	C	2	2.885(7)	0.001(1)		

^a Coordination number. ^b Interatomic distance. ^c Debye-Waller factor, s = root-mean-square internuclear separation. ^d R factor is defined as $(\int |\chi^E - \chi^T|^2 dk / \int |\chi^E|^2 dk) \times 100\%$, where χ^T and χ^E are theoretical and experimental EXAFS and k is the photoelectron wave vector.

EXAFS and crystal data is also observed for $[\text{Rh}(\text{cod})\text{Cl}]_2$ in the spectrum of which the cod group and the two bridging chlorine atoms are clearly observable.²⁴ Further afield is the other rhodium atom from this dimeric compound observable at about 3.52 Å.

The main peak in the spectrum of unsupported **1** comprises four carbon atoms from the cod ligand and of the three phosphorus atoms from the tripodal ligand (Figure 7a). The cod group is ~ 0.03 Å further away from the Rh center than in $[\text{Rh}(\text{cod})\text{Cl}]_2$, consistent with the greater trans influence of the P donors as compared to $\mu\text{-Cl}$ as well as the fact that, in the zwitterionic complex, the positive charge is localized on the Rh atom (Table 3a).

Notably, the Rh–P distances in **1** are quite coincident with those [2.367(1)_{av} Å] obtained by X-ray methods for [(tripod)-Rh(cod)]BPh₄ where tripod is the tripodal ligand PhCH₂C(CH₂-PPh₂)₃ differing from sulfos only for having a benzyl substituent in the place of the sulfonated-benzylic tail.^{20d} The Rh–C(cod)-bonding distances in the tripod complex, ranging from 2.206-(4) to 2.254(4) Å, are slightly longer than those in the sulfos derivative **1** (2.135(3) Å).

Interestingly, the spectrum of **1/SiO₂** (Figure 7b) is very similar in appearance to that of the unsupported sample (Figure 7a). Only two shells of atoms are detectable here, however. Four equidistant cod atoms are observable as are three phosphorus atoms (Table 3b). Both bond lengths from the rhodium are

(24) (a) Ibers, J. A.; Snyder, R. G. *Acta Crystallogr.* **1962**, *15*, 923. (b) Boeyens, J. C. A.; Denner, L.; Orchard, S. W.; Rencken, I.; Rose, B. G. S. *Afr. J. Chem.* **1986**, *39*, 229. (c) De Ridder, D. J. A.; Imhoff, P. *Acta Crystallogr.* **1994**, *50*, 1569.

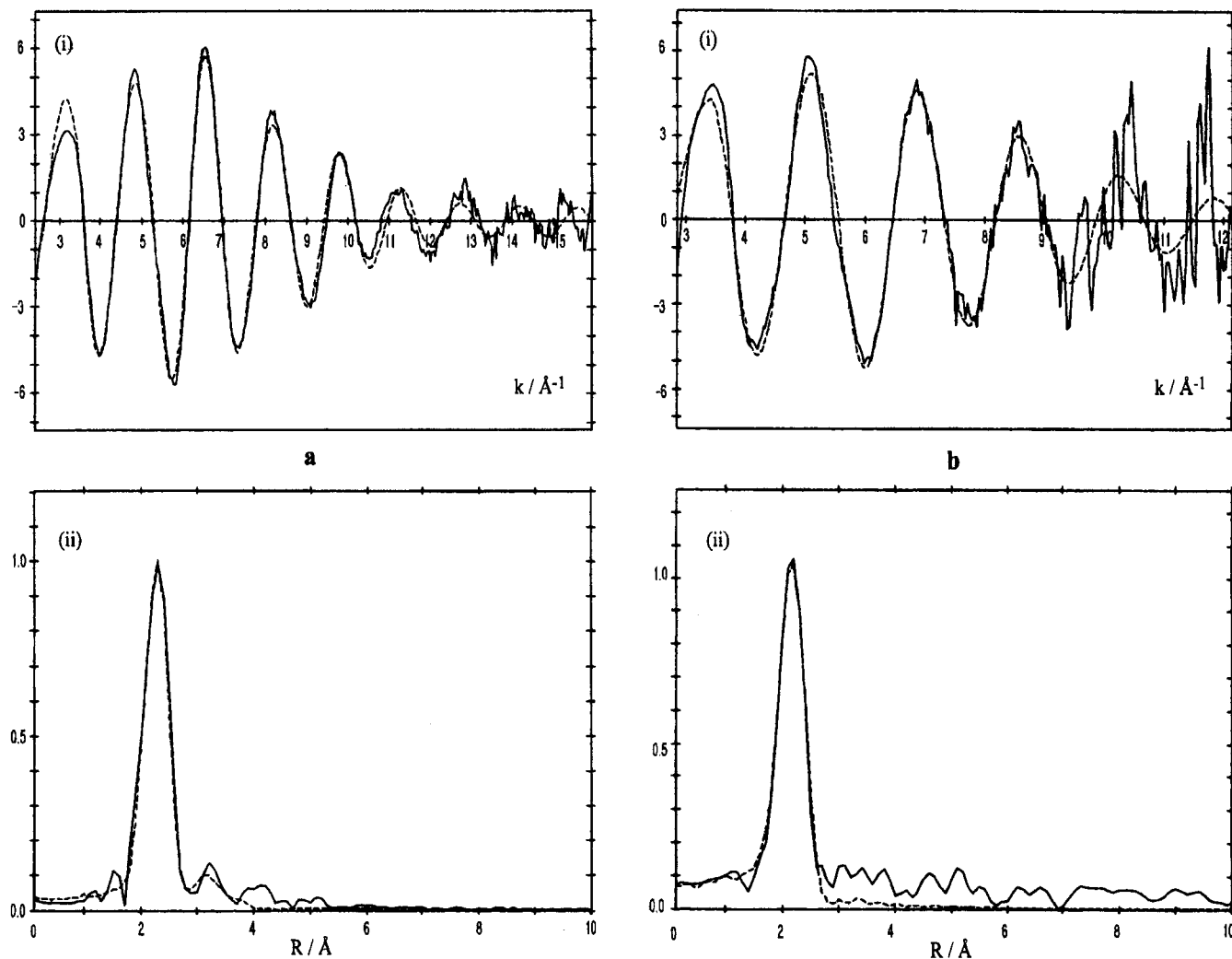


Figure 7. Rh K-edge k^3 -weighted EXAFS (i) and Fourier Transform (ii) spectra of the following: (a) pure **1** and (b) **1**/ SiO_2 ; (—) experiment and (---) spherical wave theory.

shortened by approximately 0.1 Å. This is probably related to the bonding of the organometallic to the surface.

Since the chemical environment in the vicinity of the rhodium atom in **1**/ SiO_2 is almost identical to that of pure **1**, one may again conclude that the organometallic complex is tethered to the surface OH groups using polar groups far away from the metal coordination sphere. The best candidates for this hydrogen-bonding interaction are the oxygen atoms of the sulfonate tail. Indeed, it is generally agreed that hydrogen bonding of the hydrated sodium sulfonate groups to the OH groups present at the surface of silica is responsible for the immobilization of triphenylphosphine trisulfonate complexes.^{5,25} The potential for hydrogen bonding of different forms of silica is well-known. Both experimental (IR, NMR)²⁶ and theoretical²⁷ studies indicate that the preferred adsorption sites of the hydrogen-bonded substrates are the isolated silanol groups on the surface.

TPRD Analysis. The anchored catalyst **1**/ SiO_2 was subjected to a TPRD analysis in the presence of a dihydrogen flow (Figure 8). In the temperature range 50–150 °C, with a maximum evolution peak at 100 °C, the cod ligand was completely

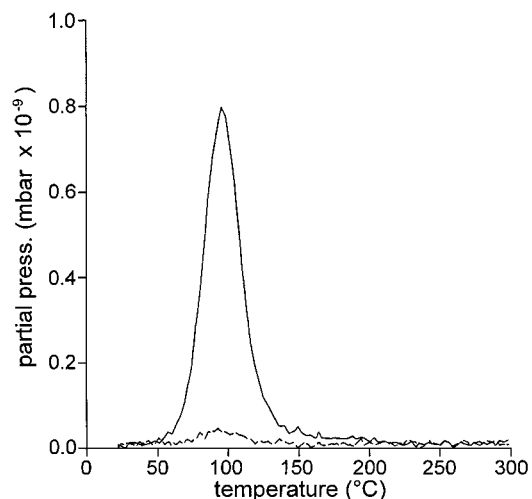


Figure 8. TPRD spectra of **1**/ SiO_2 in H_2 flow; (---) $m/z = 110$ (cyclooctene), (—) $m/z = 112$ (cyclooctane).

hydrogenated and ultimately removed as cyclooctane with traces of cyclooctene. Neither the formation of other species nor the sublimation of the complex was detected up to 300 °C.

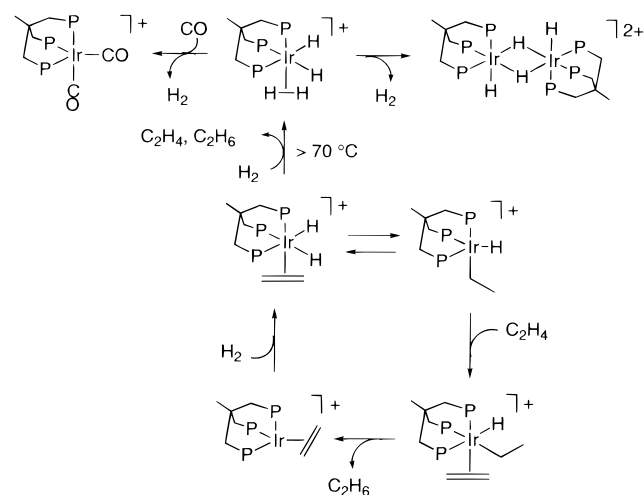
Solid–Gas Hydrogenation and Hydroformylation of Ethene and Propene. The catalytic potential of **1**/ SiO_2 in solid–gas conditions was investigated for the hydrogenation and the

(25) (a) Horváth, I. T. *Catal. Lett.* **1990**, *6*, 43. (b) Fache, E.; Mercier, C.; Pagnier, N.; Despeyroux, B.; Panster, P. *J. Mol. Catal.* **1993**, *79*, 117.

(26) Knözinger, H. In *The Hydrogen Bond. Recent Developments in Theory and Experiment*; Schuster, P., Zundel, G., Sandorfy, C., Eds.; North-Holland: Amsterdam, The Netherlands, 1976; p 1263.

(27) Hobza, P.; Sauer, J.; Morgeneyer, C.; Hurich, J.; Zahradnik, R. *J. Phys. Chem.* **1981**, *85*, 4061.

Scheme 1



hydroformylation of ethene and propene under reaction conditions comparable to those generally employed for highly dispersed Rh/SiO₂ catalysts derived from carbonyl cluster precursors.²⁸

A first attempt was made by heating a sample of 1/SiO₂ at 120 °C in a flow of argon before admitting the reaction mixtures (H₂–C₂H₄(C₃H₆) = 1:1; CO–H₂–C₂H₄(C₃H₆) = 1:1:1, respectively) at the same temperature. This treatment was necessary to have a stable temperature in the catalytic bed. Neither hydrogenation to ethane (propane) nor hydroformylation to C₃ (C₄) aldehydes was observed after 20 h on stream. As indicated by the TPRD experiments, a pretreatment in H₂ at 150 °C was then performed in order to remove the cod ligand as cyclooctane. After this treatment, the H₂–alkene mixtures were admitted into the reactor at 120 °C. Under these conditions, both alkenes were completely hydrogenated and no catalyst deactivation was observed after 15 h on stream. In contrast, the admission of the hydroformylation mixtures at 120 °C produced neither aldehydes nor alkanes. The grafted Rh precursor 1/SiO₂ was converted to the dicarbonyl derivative 2/SiO₂, which resulted in inactivity for solid–gas hydrogenation reactions, most likely due to the strong Rh–CO bonds as well as the difficulty to create, in the solid state, free coordination sites for either H₂ or alkenes by phosphine arm unfastening (vide infra). The incapacity of monomeric Rh complexes supported on either silica or alumina for catalyzing the hydroformylation of ethene in solid gas conditions has previously been reported by Iwasawa et al., who showed that a fundamental role in the heterogeneous process is played by adjacent Rh atoms.^{29,30}

The hydrogenation of ethene over a crystalline organometallic catalyst has recently been reported to take place in a flow reactor under mild conditions (1 bar H₂, 60 °C) with no need of a support.³¹ Remarkably, the organometallic catalyst is a triphos metal compound, namely the dihydride(ethylene) complex [(triphos)Ir(H)₂(C₂H₄)]BPh₄. The proposed solid–gas mechanism, illustrated in Scheme 1, is a typical hydrogenation cycle of alkenes catalyzed by soluble metal complexes.³² Scheme 1 also shows that the poisoning of the hydrogenation catalyst may occur in the solid state either thermally (≥70 °C) or by treatment

with CO. In the former case, the catalyst converts to the dimer [(triphos)IrH(μ-H)₂HIr(triphos)](BPh₄)₂ via a dihydride(η²-H₂) derivative,³¹ while the dicarbonyl complex [(triphos)Ir(CO)₂]-BPh₄ is formed in the presence of CO.

In light of the flow reactor and EXAFS studies (see below), it is probable that the hydrogenation of ethene or propene catalyzed by 1/SiO₂ follows a mechanism similar to that shown in Scheme 1 for [(triphos)Ir(H)₂(C₂H₄)]BPh₄. Unlike the Ir complex, however, 1/SiO₂ is an efficient hydrogenation catalyst also at high temperature because the immobilization on the silica surface impedes the dimerization to μ-hydrido species (vide infra).

EXAFS Characterization of the Grafted Rh Products after the Solid–Gas Reactions of 1/SiO₂. The EXAFS spectrum of 1/SiO₂ after the pretreatment with H₂ at 150 °C showed a very different shape (Figure 9a) than that of the supported organometallic prior to reduction (Figure 7b). The cod ligand, lost as cyclooctane, has probably been replaced by hydride species. However, since the EXAFS is incapable of identifying the hydrogen atom due to its low electron density, the presence of hydride ligands may only be hypothesized on the basis of the lengthening of the Rh–P distance (Table 3c). Indeed, the three phosphorus atoms are clearly evident at a radius greater than the previous radius, which may be due to the substitution of the cod ligand for groups with greater trans influence such as hydride ligands.³³ The other peak in the spectrum can be attributed to a carbon atom from the phenyl groups adjacent to the phosphorus atoms.

After the reaction of the preactivated silica-grafted 1/SiO₂ catalyst with the H₂–C₂H₄ mixture at 120 °C, the EXAFS spectrum showed that a variety of carbon atoms were bonded to the rhodium atom, while the phosphorus atoms from the sulfos ligand were unchanged (Figure 9b). On the basis of their distances to rhodium (Table 3d),³⁴ the carbon atoms are tentatively assigned to both alkyl and alkene species as in one of the intermediates proposed for the solid–gas hydrogenation of ethene with the Ir complex [(triphos)Ir(H)₂(C₂H₄)]BPh₄ (Scheme 1).

In all cases, there was no indication of the formation of contiguous Rh–Rh sites, indicating that the catalytic active sites are isolated Rh atoms, as in homogeneous phase. This finding is quite interesting as site–site isolation is not guaranteed by immobilization of a metal complex on silica.^{35a}

Solid–Liquid Hydrogenation of Styrene and Hydroformylation of 1-Hexene. The catalytic performance of the supported Rh complexes in liquid–solid conditions was tested in the hydrogenation of styrene and in the hydroformylation of 1-hexene just to make a comparison with analogous reactions catalyzed by the unsupported counterparts in liquid-phase systems.¹

(32) Collman, J. P.; Hegedus, L. S.; Norton, J. R.; Finke, R. G. *Principles and Applications of Organotransition Metal Chemistry*; University Science Books: Mill Valley, CA, 1987; Chapter 10, p 523.

(33) (a) Appleton, T. G.; Clark, H. O.; Manzer, L. E. *Coord. Chem. Rev.* **1973**, *10*, 335. (b) Mason, R.; Meek, D. W. *Angew. Chem., Int. Ed. Engl.* **1978**, *17*, 183, and references therein. (c) Collman, J. P.; Hegedus, L. S.; Norton, J. R.; Finke, R. G. *Principles and Applications of Organotransition Metal Chemistry*; University Science Books: Mill Valley, CA, 1987; Chapter 4, p 242.

(34) Orpen, A. G.; Brammer, L.; Allen, F. H.; Kennard, O.; Watson, D. G.; Taylor, R. *J. Chem. Soc., Dalton Trans.* **1989**, S1.

(35) (a) Collman, J. P.; Belmont, J. A.; Brauman, J. I. *J. Am. Chem. Soc.* **1983**, *105*, 7288. (b) Andersen, J.-A. M.; Currie, A. W. S. *J. Chem. Soc., Chem. Commun.* **1996**, 1543. (c) Cornils, B.; Herrmann, W. A. In *Applied Homogeneous Catalysis with Organometallic Compounds*; Cornils, B., Herrmann, W. A., Eds.; VCH: Weinheim, Germany, 1996; Vol. 2, p 575.

(28) Fusi, A.; Psaro, R.; Dossi, C.; Garlaschelli, L.; Cozzi, F. *J. Mol. Catal.* **1996**, *107*, 255.

(29) Asakura, K.; Kitamura-Bando, K.; Iwasawa, Y.; Arakawa, H.; Isobe, K. *J. Am. Chem. Soc.* **1990**, *112*, 9096.

(30) Kitamura-Bando, K.; Asakura, K.; Arakawa, H.; Isobe, K.; Iwasawa, Y. *J. Phys. Chem.* **1996**, *100*, 13636.

(31) Bianchini, C.; Farnetti, E.; Graziani, M.; Kaspar, J.; Vizza, F. *J. Am. Chem. Soc.* **1993**, *115*, 1753.

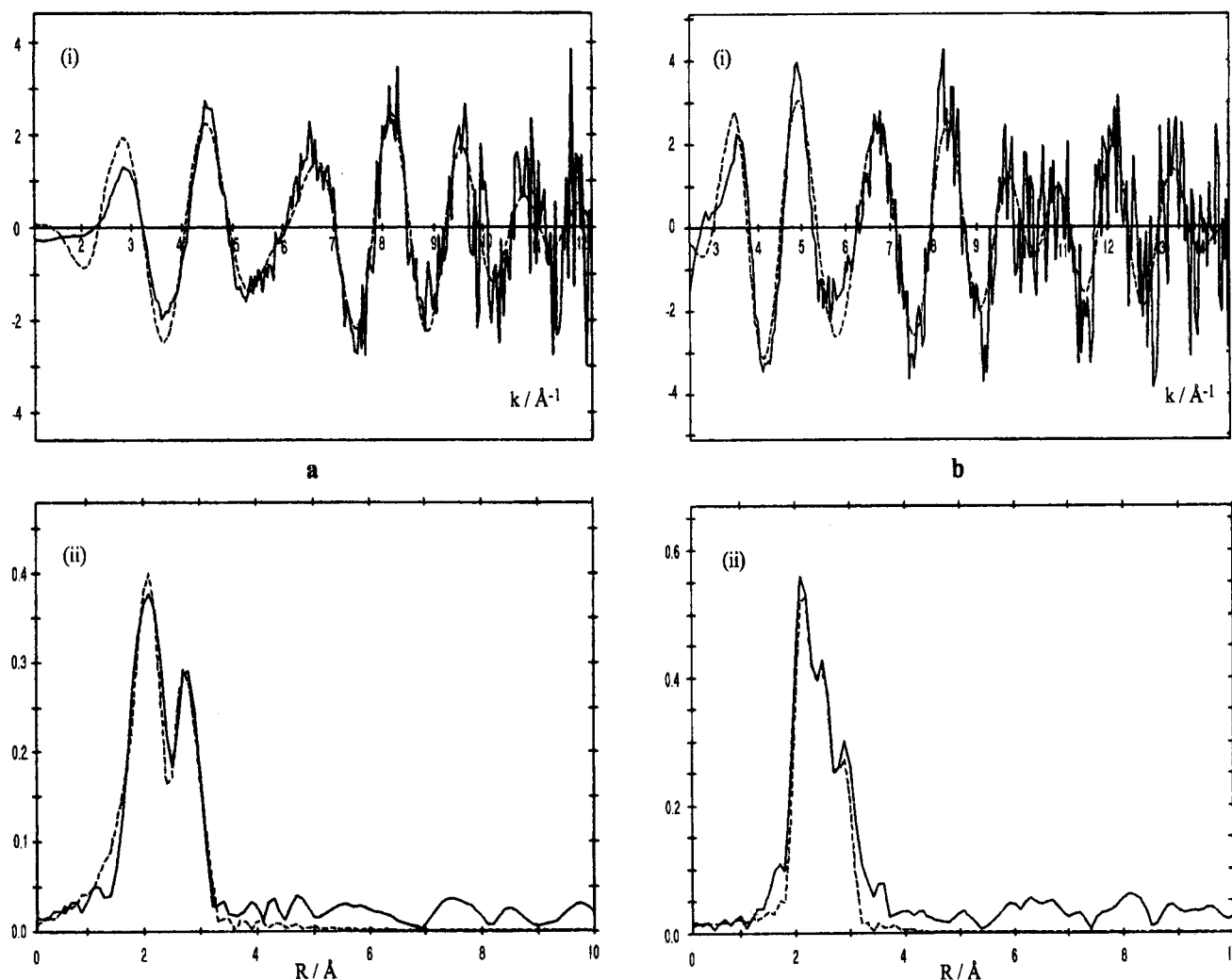


Figure 9. Rh K-edge k^3 -weighted EXAFS (i) and Fourier Transform (ii) spectra of the following: (a) $1/\text{SiO}_2$ after activation in H_2 flow at 150°C ; (b) activated $1/\text{SiO}_2$ after reaction with $\text{H}_2\text{C}_2\text{H}_4$ mixture at 120°C ; (—) experiment and (---) spherical wave theory.

In the presence of $1/\text{SiO}_2$ suspended in a hydrocarbon solvent, styrene was completely converted to ethylbenzene while 1-hexene, at 100% conversion, was hydroformylated to a mixture of heptanal (32.0%), 2-methylhexanal (41.0%), and 2-ethylpentanal (15.5%). The rest of 1-hexene was isomerized to internal alkenes with a little hydrogenation product (3.5%). Following the hydrogenation reaction, the cod ligand in the catalyst precursor was quantitatively converted to cyclooctane, whereas it was partially hydrogenated to cyclooctene in the hydroformylation reaction, suggesting that the displacement of the olefinic end of cyclooctene by CO is much faster than hydride migration. The great propensity of CO to bind the Rh center was also demonstrated by the detection of free cod ($\sim 20\%$) in the reaction mixture after hydroformylation.

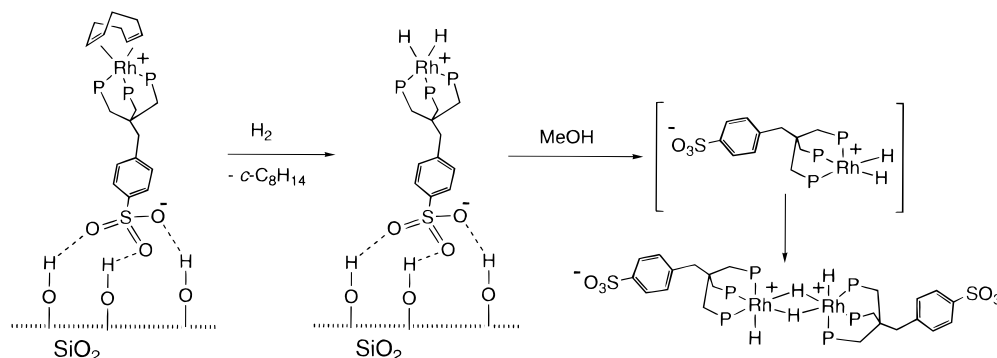
Some successful examples of alkene hydroformylations with Rh catalysts anchored to silica via covalent bonding have recently been reported with mono- and diphosphine ligands.³⁵ In general, a drawback to these systems, particularly to those comprising monodentate phosphines, is an appreciable rhodium leaching under high pressure of CO. A tripodal tridentate phosphine such as sulfos is expected to be less prone to catalyst leaching and, indeed, both the hydrogenation and hydroformylation reactions with the present SHB catalysts proceeded with no leaching as determined by atomic absorption analysis of both the hydrocarbon solvent and the supported material after this was filtered off and washed with *n*-octane and then with $\text{CH}_2\text{-}$

Cl_2 . The recovered catalysts were reused in hydrogenation and hydroformylation reactions, yielding unchanged conversions and product compositions, whereas no catalytic activity was observed using the filtrates.

As compared to the analogous liquid-biphase reactions catalyzed by **1** and **2** in MeOH –water–*i*-octane at 80°C ,¹ the solid–liquid hydroformylation reactions gave a major chemoselectivity as no trace of C_7 alcohols was detected. The conversion to aldehydes was also higher using the silica-grafted catalyst (88% vs 54%), while the linear–branched ratio was much lower in the solid–liquid reaction (0.6) than in the liquid-biphase one (2.2). In truly homogeneous phase (THF solvent), the catalyst precursor [(triphos)Rh(dmad)] BPh_4 (dmad = dimethylacetylene dicarboxylate) gave lower productions of aldehydes (20% at 60°C ; 34% at 100°C) with linear–branched ratios varying from 1.7 at 60°C to 4.1 at 100°C .^{19d} The transformation of the mononuclear Rh precursor into binuclear species with bridging hydride ligands was proposed to be the factor responsible for the low catalytic activity in solution. The remarkable efficiency of the grafted complexes may thus be ascribed to the fact that the active sites are isolated Rh species all over the hydroformylation reaction.

To provide experimental evidence of the formation of Rh–H moieties after the hydrogenation of $1/\text{SiO}_2$, we subjected the grafted cod complex suspended in *n*-octane to 30 bar of H_2 at 120°C for 1 h in the Parr autoclave. After separation from the

Scheme 2



hydrocarbon solution containing cyclooctane, the grafted Rh product was extracted from the silica with a 1:2 mixture of MeOH and MeOH-*d*₄. A ³¹P{¹H} NMR analysis of the yellow–orange methanol solution showed the presence of a doublet at δ 24.5 ($J(\text{PRh}) = 88$ Hz) and of a singlet at δ 32.4 with no evident P–Rh coupling and readily assignable to P=O phosphorus nuclei. The doublet signal is highly reminiscent of a tetrahydrido dimeric structure as in $[(\text{triphos})\text{RhH}(\mu\text{-H})_2\text{HRh}(\text{triphos})]^{2+}$ (δ 25.2, $J(\text{PRh}) = 90$ Hz) obtained by protonation of the trihydride $(\text{triphos})\text{RhH}_3$.³⁶ Consistently, an unresolved signal at δ about -10 was seen in the ¹H NMR spectrum. On standing, the yellow–orange MeOH-*d*₄ solution turned red–brown and the doublet signal at δ 25.5 decreased in intensity to disappear within 2 h. Again, this behavior is reminiscent of the spontaneous transformation in alcohols of the yellow–orange diamagnetic complex $[(\text{triphos})\text{RhH}(\mu\text{-H})_2\text{HRh}(\text{triphos})]^{2+}$ into the red, paramagnetic dimer $[(\text{triphos})\text{Rh}(\mu\text{-H})_3\text{Rh}(\text{triphos})]^{+}$ (Scheme 2).³⁷ Qualitative identification of the rhodium complex extracted from the silica was also carried out by IR spectroscopy. After methanol was eliminated under reduced pressure, the IR spectrum (Nujol mull, KBr plates) showed a $\nu(\text{Rh-H})$ band at 1970 cm^{-1} which matches well the value reported for the terminal Rh–H bonds in the complex cation $[(\text{triphos})\text{RhH}(\mu\text{-H})_2\text{HRh}(\text{triphos})]^{2+}$.³⁷

Following a similar procedure, the supported material after a hydroformylation run was filtered off and the grafted metal species was extracted with methanol. NMR and IR analysis of the yellow–orange solutions gave evidence of the formation of the dicarbonyl complex **2**.

As already commented, the absence of catalytic activity shown by the grafted complexes in the solid–gas hydroformylation reaction may be ascribed to the strong coordination of CO combined with the apparent incapability of unfastening a phosphine arm in the solid state without the cooperation of a liquid phase. Indeed, intermediate species with η^2 -triphos ligands have invariably been proposed to rationalize the mechanisms of the hydroformylation reactions catalyzed by triphos metal precursors.^{19d,20b,38} In contrast, the hydrogenation reactions of alkenes with triphos metal catalysts do not require the decoordination of a phosphorus donor at any stage of the process.^{19d}

Conclusions

The present study introduces a facile and clean method of preparing immobilized polyphosphine metal catalysts, denoted

SHB catalysts, for use in both solid–gas and solid–liquid reactions in hydrocarbon solvents. The procedure involves a hydrogen-bonding interaction between the silanol groups of the support and a sulfonate group far away from the phosphorus donor atoms of the ligands. In this way, all of the metal centers are potential reagents dispersed on a very high interfacial area. Moreover, in all the cases investigated there was no evidence whatsoever of the formation of contiguous Rh–Rh sites, indicating that the catalytic active sites are isolated Rh atoms, as in homogeneous phase.

Despite the $-\text{SO}_3\cdots\text{HOSi}-$ interaction not being as chemically robust as the covalent bonding commonly employed to immobilize organometallic complexes of wide use in heterogeneous catalysis,^{35,39} the SHB complexes prove extremely versatile, thermally robust, and easily recycled hydrogenation or hydroformylation catalysts. Studies in progress show that a variety of unsaturated substrates can efficiently be hydrogenated or carbonylated by the SHB catalysts under mild conditions in hydrocarbon solvents.

A further interesting feature of SHB catalysis is provided by the facile and quantitative extraction of the grafted metal products with alcohols. This allows one to study the metal products of single site catalytic reactions applying standard spectroscopic techniques in solution as occurs when the heterogenization of organometallic complexes is achieved by the ion pairing technique.⁴⁰

The heterogenization method described here may also be seen as an alternative to SAP catalysis in which the immobilization requires a thin surface water film on the support.⁵ The use of water obviously limits the variety of complexes to be immobilized as they must be water-soluble and possibly contain cations (generally the sodium ions of the sulfonated phosphine ligands) to provide a strong electrostatic contribution to the overall bonding interaction, catalyst–water–support. In addition, SAP catalysis cannot be applied to reactions in which reagents and products react undesirably with water.

Acknowledgment. A contract (PR/1) from the Ministero dell' Ambiente di Italy is gratefully acknowledged for financial support. The support of the Istituto Nazionale di Coordinamento sulle Metodologie e Tecnologie Chimiche Innovative of CNR is also acknowledged. The authors thank Daresbury Synchrotron Radiation Laboratories and the ESRF (Grenoble) for the

(36) Bianchini, C.; Meli, A.; Laschi, F.; Ramirez, J. A.; Zanello, P. *Inorg. Chem.* **1988**, *27*, 4429.

(37) Bianchini, C.; Laschi, F.; Masi, D.; Mealli, C.; Meli, A.; Ottaviani, F. M.; Proserpio, D. M.; Sabat, M.; Zanello, P. *Inorg. Chem.* **1989**, *28*, 2552.

(38) Kiss, G.; Horváth, I. T. *Organometallics* **1991**, *10*, 3798.

(39) (a) Hanson, B. E. In *Encyclopedia of Inorganic Chemistry*; King, R. B., Ed.; John Wiley: New York, 1994; Vol. 7, p 4056. (b) Carpentier, J.-F.; Agbossou, F.; Mortreux, A. *Tetrahedron* **1995**, *6*, 39. (c) Gao, H.; Angelici, R. J. *J. Am. Chem. Soc.* **1997**, *119*, 6937.

(40) Roberto, D.; Cariati, E.; Pizzotti, M.; Psaro, R. *J. Mol. Catal.* **1996**, *111*, 97, and references therein.

provision of synchrotron radiation and the staff of Station 9.2 and GILDA for technical assistance, respectively. EPSRC is also thanked for research studentship (to D.B.). Thanks are due to Julian Grimshaw (University of Southampton) and Dr.

Claudia Forte (ICQEM-CNR, Italy) for the assistance in recording the CP MAS ^{31}P NMR spectra.

JA983940G